PTEN Hypomethylation Could Be A Biomarker For Early Detection of Silicosis

Weijiang Hu
Chinese Center for Disease Control and Prevention, Beijing 100050, China
Jingbo Zhang
Tongji University School of Medicine
Kai Liu
Chinese Center for Disease Control and Prevention, Beijing 100050, China
Jie Liu
Department of Occupational Disease
Yuxin Zheng
Qingdao University
Xin Sun
Chinese Center for Disease Control and Prevention, Beijing 100050, China
Liangying Mei
Hubei Provincial Center for Disease Control and Prevention
Zushu Qian
Huangshi Center for Disease Control and Prevention
Qiangguo Sun
Huangshi Center for Disease Control and Prevention
Qiang Liu
Suzhou Center for Disease Control and Prevention
Zhijun Wu
Chinese Center for Disease Control and Prevention
Hengdong Zhang
Jiangsu Provincial Center for Disease Control and Prevention
Yanping Li
Honghe Prefecture Third People's Hospital
Daoyuan Sun (dysun@163.com)
Tongji University School of Medicine
Meng Ye
Chinese Center for Disease Control and Prevention

Research Article

Keywords: PTEN Methylation, miRNAs, mRNAs, silicosis, biomarker, early detection

Posted Date: November 12th, 2021

DOI: https://doi.org/10.21203/rs.3.rs-1038220/v1

Abstract

The overwhelming majority of subjects in current silicosis mRNA and miRNA expression profile are of human blood, lung cell, or rats model, which put limit on understanding of silicosis pathogenesis and therapy. It is essential to identify differentially expressed mRNAs and miRNAs profiles in silicosis patients lung tissues, and explore potential biomarker for early detection of silicosis. So we conducted a transcriptome study based on fifteen silicosis patients and eight normal people lung tissues, meanwhile, we validated the predictions with 404 silicosis patients and 177 normal people blood samples. The results showed that 1417 and 241 differentially expressed mRNAs and miRNAs were identified, respectively, among normal people, early stage silicosis, and advanced silicosis lung tissues (all P values < 0.05), whereas there were no significant difference in most mRNAs or miRNAs expression between early stage and advanced stage silicosis lung tissues. Enrichment analysis indicated phagosome, ribosome, olfactory transduction, antigen processing and presentation and PI3K-Akt pathways were mainly involved in the onset of silicosis. Series test of cluster (STC) analysis segregated differentially expressed mRNAs and miRNAs into five and three expressopm profiles patterns, repectively, with significant trends (P < 0.05), meanwhile, ten mRNAs (PIK3R3, KRAS, CTNNB1, HIF1A, ITGA2, KIT, SOCS3, GNAI3, STAT3 and PTEN) and nine miRNAs (hsa-miR-27a-3p, hsa-miR-27b-3p, hsa-miR-34b-3p, hsa-miR-3613-3p, hsa-miR-575, hsa-miR-8063, hsa-miR-937-5p, hsa-miR-181a-5p and hsa-miR-181b-5p) in patterns with opposite trends were selected to make further RT-qPCR validation in lung tissues and blood samples. Finally, the lung tissues RT-qPCR results verified microarray analyses of mRNAs and miRNAs expression trends, except for hsa-miR-575, hsa-miR-8063, and hsa-miR-937-5p, whereas blood samples RT-qPCR results PTEN and GNAI3 had opposite expression trends to those of lung tissues, and PTEN was identified as potential biomarker for silicosis early detection due to low methylation in the blood.

Introduction

Globally, 39% of total pneumoconiosis cases were ascribed to silicosis in 2017[1]. The silicosis is mainly caused by excessive inhalation of silica dust which, over time, leads to lung inflammation and fibrosis[2]. Besides, dysregulated mRNAs and miRNAs are implicated in immune response and inflammation[3], and differences in mRNAs and miRNAs expressions between silicosis and normal subjects have been reported in many studies[4-10]. However, most subjects of current silicosis related transcriptome studies concentrate mainly on human blood[6, 7], bronchoalveolar lavage fluid[4], macrophages[9], lung epithelial cells[8], or rats model[10-12] instead of silica dust major target organ-human lung tissue. In addition, despite the same silicosis rats model, the numbers of differential mRNA or miRNA expression were still controversial[5, 10, 13, 14]. Hence, it is critical and essential to conduct a transcriptome study based on silicosis patients and normal people lung tissues. Our previous study revealed that PTEN promoter hypermethylation might be associated with decrease of PTEN protein in silicosis lung tissues[15], whereas its expression profile in silicosis patients blood samples was still unclear.

Herein, we reported a transcriptome study based on fifteen silicosis patients and eight normal people lung tissues, and made further quantitative real-time PCR (RT-qPCR) validation in other ten lung tissues and

581 blood samples. Our study provides detailed differential mRNAs and miRNAs expressions, and highlights the great significance of exploring silicosis underlying toxicological mechanisms in lung tissues.

Methods

Lung tissues and blood samples of silicosis patients and normal people

Silicosis patients and normal people lung tissues were obtained from National Institute for Occupational Health and Poison Control, Chinese Center for Disease Control and Prevention. We selected patients with silicosis who had undergone autopsying between 1967 and 1979, whereas cases combined with lung cancer or other pulmonary diseases were excluded. In addition, cases were divided into early stage group and advanced stage group according to diagnosis of occupational silicosis: early stage group included stage Ⅰ; advanced stage group included stage Ⅱ and Ⅲ[15, 34]. A total ofsix early stage silicosis cases, nine advanced stage silicosis cases, and eight normal lung tissues were included for microarray processing, and RT-qPCR validation.

Besides, blood samples of 414 male silicosis patients and 177 male normal people were collected for further RT-qPCR validation during 2015. The silicosis patients, diagnosed according to GBZ 70-2009, were selected from two silica dust-exposed enterprises: 353 of one copper mine, and 61 of one stone processing factory. 177 normal people were selected as control group from one local food processing company. The cases inclusion criteria were: 1) occupational silica dust exposure; 2) diagnosed silicosis according to GBZ 70-2009; and 3) no other occupational dust exposure except for silica dust. The control samples inclusion criteria were: 1) no occupational dust exposure; 2) no cancer; 3) no pulmonary fibrosis under imaging examination; and 4) no hereditary lung diseases. Finally, a total of 404 silicosis patients and 177 normal people blood samples were included.

All the lung tissues and blood samples were obtained through the medically prescribed test, including informing each participant, and written informed consent was obtained from all subjects. Meanwhile, this study was approved by the Ethics Committee Board in Occupational Health and Poison Control, Chinese Center for Disease Control and Prevention. Within ten minutes after sampling, lung tissue and blood samples were stored at -80℃ refrigerator. The main clinical characteristics of silicosis patients and normal people were presented in Supplementary Table 21 and Supplementary Table22: Supplementary Table 21 of lung tissues, and Supplementary Table 22 of blood samples. Furthermore, there were no statistically significant differences in the age, gender, and smoking between silicosis patients and normal people in Supplementary Table 21 or Supplementary Table 22.

Microarray Processing And Analyses

RNA preparation Three early stage silicosis, five advanced silicosis, and four normal lung tissues were randomly selected for microarray processing and analyse.The total RNA in lung tissues was extracted using Trizol Reagent (Invitrogen, Carlsbad, Canada), and purified with an RNeasy Mini Kit (Qiagen, Hilden, Germany) according to the manufacture's protocol, including a DNase digestion treatment. The amount and quality of RNA were determined by a UV-Vis Spectrophotometer (Thermo, NanoDrop 2000, USA) at the absorbance of 260 nm.

miRNA microarray processiong The miRNA microarray profiling was performed using GeneChip® miRNA 4.0 Array (Santa Clara, CA, USA) according to manufacturer's recommended protocol. Briefly, 1 μg of total RNA from samples was labeled by polyA polymerase using the Genisphere FlashTag HSR kit according to the manufacture's recommendations (Genisphere, Hatfield, PA). In addition, RNA was hybridized to the Affymetrix miRNA array as recommended by the vendor. Standard Affymetrix array cassette staining, washing and scanning was performed using the post-hybridization kit (#900720; Affymetrix) and GeneChip Scanner 3000. Feature extraction was performed using Affymetrix Command Console software. Furthermore, the raw data were treated by the following workflow: background detection, RMA global background correlation, quantile normalization, median polish and log2-transformed with miRNA QC tool software (Affymetrix).

mRNA microarray processiong The mRNA expression profiling was measured using GeneChip Human Transcriptome Array 2.0 (Affymetrix GeneChip, Santa Clara, CA, USA), which contained 59, 302 gene-level probe sets.The microarray analysis was performed by Affymetrix Expression Console Software (Version 1.2.1). Raw data (CEL files) were normalized at transcript level using robust multi-array average method (RMA workflow). Median summarization of transcript expression was calculated. Mrna expression data were then filtered to include only those sets that were in the 'core' metaprobe list, which represented RefSeq genes.

Differentially expressed RNAs (DERs)analyses and heatmap generating Given the random-variance model *F*-test can raise degrees of freedom effectively in the cases of small samples, it was applied to filter the differentially expressed RNA among early stage, advanced stage and control groups. The significance criteria of DERs was *P*-value < 0.05, and heatmaps of DERs were generated using the online tool Morpheus. Furthermore, fold change (FC) was calculated as geom mean of probeset intensities in case group divided by that of control group, and differential expressions of mRNA and lncRNA amongnormal, early stage, and advanced stagelung tissues were identified by fold change (FC) > 2.00 or < 0.50: FC > 2.00 indicated up-regulate, and FC < 0.50 indicated down-regulate.

Gene Ontology (Go) And Pathway Analyses

The above differentially expressed mRNAs were further used to conduct Gene ontology (GO) and pathway analyses. GO analysis was applied to analyze the main function of the differential expression mRNAs according to the Gene Ontology, which could organize mRNAs into hierarchical categories and uncover the mRNAs regulatory network on the basis of biological process and molecular function.

Pathway analysis was used to find out the significant pathway of the differential genes according to Kyoto Encyclopedia of Genes and Genomes (KEGG).

mRNA-mRNA-network

mRNA-mRNA interaction network was constructed based on the data of differentially expressed mRNAs to identify key mRNAs (betweenness centrality > 0.05 and degree ≥ 6). In network, the degree measured how correlated a gene was with all other network mRNAs. For a mRNA in the network, the number of source mRNAs of a mRNA was called the indegree of the mRNA, and the number of target mRNAs of a mRNA was its outdegree. The character of mRNAs was described by betweenness centrality measures reflecting the importance of a node in a graph relative to other nodes.

Series test of cluster (STC) and STC-GO analyses

STC analysis was performed using normal, early stage and advanced stage lung tissues to explore possible changes in differentially expressed mRNAs and miRNAs expression patterns during the process of silicosis. Therefore, we set 16 distinct and representative significant model profiles for the above mRNAs and miRNAs, respectively. Given that there might be a large amount of significant trends, we selected mRNAs in patterns with opposite trends to those of miRNAs expression patterns to conduct further analyses. Furthermore, mRNAs and miRNAs in patterns with the completely opposite trends and significance were selected to conduct network analysis; mRNAs and miRNAs in patterns with opposite trends and more significant differences were selected to make RT-qPCR validation.

miRNAs target mRNAsand the intersecting mRNAs

The miRNAs in pattern with a completely opposite trend to mRNAs expression pattern were used to predict their target mRNAs by miRanda, and the intersecting mRNAs were extracted between the above target mRNAs and those mRNAs in pattern with an opposite trend to miRNAs expression pattern.

miRNA-mRNA-network

miRNA-mRNA interaction network was constructed based on the data of intersecting mRNAs and miRNAs, which were in pattern with an opposite trend to mRNAs expression pattern, according to their interactions in the Sanger miRNA database. Besides, the center of this network was represented by degree, which was the contribution of one miRNA to the mRNAs around or the contribution of one mRNA to the miRNAs around, and the key miRNA and mRNA in the network always had the biggest degrees.

RT-qPCR validation

RNA preparation The blood samples and remaining lung tissues, including three early stage silicosis, four advanced stage silicosis, and three normal lung tissues, were used to make RT-qPCR. Moreover, the above seven silicosis lung tissues were considered as case group, and other three normal lung tissues as control group. Quantitative real-time PCR was performed using SYBR Green assays (ABI,7500Fast), including primers synthesized by CNKINGBIO (Beijing, China) (Supplementary Table 23 and Supplementary Table 24), and β-actin was used as an internal control.

RT-qPCR validation in lung tissues According to mRNA-mRNA-network, STC, and mRNA-miRNA-network analyses results, a representative set of ten mRNAs (Supplementary Table 23) and nine miRNAs (Supplementary Table24) were selected to make RT-qPCR validation. The above ten mRNAs were in pattern with more significant difference and opposite trend to that of miRNA expression profile. In addition, among the above ten mRNAs and nine miRNAs, nine mRNAs had high degrees (degree > 6) in mRNA-mRNA-network, and PTEN was selected given our previous study[15]; and the nine miRNAs were under selected mRNAs directed interactions.

RT-qPCR validation in blood samples Based on the above RT-qPCR validation results in lung tissues and previous studies[15, 35-38], PTEN and GNAI3, as well as hsa-miR-8063 and hsa-miR-181b-5p which regulated PTEN (Supplementary Table9to 12) were selected as markers for further validation in an independent cohort of 404 silicosis patients and 177 normal people blood samples.

Bisulfite Sequencing PCR (BSP)

Accoding to the above RT-qPCR results, PTEN, an important tumor suppressor gene, had completely opposite expression levels between lung tissues and blood samples. So bisulfite sequencing PCR was used to detect PTEN methylation state change in case group and control group blood samples. PTEN was extracted using the Genomic DNA Purification Kit (Promega, Madison, WI, USA) based on randomly selected control and case groups blood samples. In addition, 1 μg PTEN was treated with bisulfite using EpiTect Fast Bisulfite Conversion Kit (Cat No. 59824, Qiagen, Hilden, Germany) as follows: bisulfite conversion of PTEN, purification of converted PTEN, primer design, and PCR amplification of bisulfite-converted PTEN. Furthermore, the BSP specific primers were designed according to the location of the target genes CpG islands (Supplementary Table 25 and Supplementary Text).

Statistical Analyses

Random-variance model *F*-test was applied to filter the differentially expressed RNAs, and differential expression RNAs were selected at a logical sequence according to RVM (Random variance model) corrective ANOVA. Besides, the significant GO and pathway categories were examined by Fisher's exact test and χ^2 test. The criteria of significance was defined by *P*-value < 0.05. The above statistical analyses were performed using SPSS 23.0 (SPSS Inc., Chicago, IL, USA).

Results

Differentially expressed mRNAs and miRNAs in silicosis patients and normal people lung tissues

According to quality-control tests results, there was one early stage silicosis lung tissue excluded due to no detection in mRNA microarray processing. Therefore, a total of eleven and twelve lung tissues included in mRNA and miRNA microarray analyses, respectively: seven and four of case and control groups, respectively, in mRNA microarray analysis; eight and four of case and control groups, respectively, in miRNA microarray analysis. As a result, we totally identified 1417 differentially expressed mRNAs (Fig. 1a;Supplementary Table 1 and Supplementary Table 2), and 241 differentially expressed miRNAs (Fig. 1b;Supplementary Table 1 and Supplementary Table 2) among normal, early stage silicosis and advanced silicosis lung tissues. Given that most mRNAs or miRNAs expressions had no significant difference between early stage and advanced stage silicosis lung tissues, lung tissues or blood samples from early stage and advanced stage silicosis patients were considered as case group in further analyses, except series test of cluster (STC) analysis.

GO and pathway analyses

On the basis of above results, we conducted gene ontology (Go) and pathway analyses to analyze main functions and find out significant pathways of differential expression mRNAs. The GO results indicated that differentially expressed mRNAs were closely related to gene expression, viral reproduction, viral infectious cycle functions, and etc (Supplementary Fig. 1a,Supplementary Table 3 and 4). In addition, these differential expression mRNAs were enriched in phagosome, ribosome, olfactory transduction, antigen processing and presentation, PI3K-Akt pathways, and etc (Supplementary Fig. 1b,Supplementary Table 5). Notably, an unexpected discovery was silica-exposure induced differentially expressed mRNAs involving in proteoglycans in cancer and pathways in cancer, and mRNAs included PIK3R3, HIF1A, FN1, FZD2, FGF18, ITGA2, MMP2, CTNNB1, CDKN1A, KRAS, STAT3, FZD4, FGF17, FGF6, ITGB1, FGF2, ITGAV, MAP2K1 (Supplementary Table 6).

mRNA-mRNA-network

To identify key mRNAs in differentially expressed mRNAs, mRNA-mRNA functional interaction network was conducted, and the result revealed nine key mRNAs: SOCS3, KIT, STAT3, FIGF, CTNNA1, PIK3R3, HIF1A, NFKB1, and TJP1 (Supplementary Fig. 2,Supplementary Table 7 and 8). Among the above nine mRNAs, SOCS3 had the highest centrality, and PIK3R3 had the highest degree value. SOCS3 expression was promoted by NFKB1, whereas inhibited by STAT3. Besides, FIGF could activate KIT, and KIT activated STAT3 and PIK3R3.

Series test of cluster (STC) and STC-GO analyses

STC analyses results showed five and three patterns of mRNAs and miRNAs expressopm profiles, repectively,with significant trends (P< 0.05) (Supplementary Table 9 to 12). Among these patterns, mRNA expression profile 5 had completely opposite trend to that of miRNA expression profile 8: mRNAs expression in mRNA expression profile 5 (Fig. 2a) increased in early stage, and reduced in advanced stage; whereas miRNAs expression in miRNA expression profile 8 (Fig. 2b) reduced in early stage, and increased in advanced stage. STC-GO analysis suggested mRNAs in expression profile 5 (Fig. 2a) were mainly involved in detection of chemical stimulus involved in sensory perception of smell, G-protein coupled receptor signaling pathway, and sensory perception of smell, etc. Besides, mRNA expression profile 3 and miRNA expression profile 13, mRNA expression profile 13 and miRNA expression profile 3 had opposite trends, respectively, with more significant differences.

miRNAs target mRNAs and the intersecting mRNAs

Based on STC analyses, miRNAs in pattern with completely opposite trend to mRNAs expression pattern were used to predict their target mRNAs by miRanda. Finally, the miRNAs in miRNA expression profile 8 were used to make further prediction, and we found 12781 target mRNAs (Supplementary Table 13). Moreover, there were 39 intersecting mRNAs extracted between the above 12781 target mRNAs and mRNAs in mRNA expression profile 5 (Fig. 2a;Supplementary Table 9 and Supplementary Table 10).

miRNA-mRNA-network

The above intersecting mRNAs and miRNAs in miRNA expression profile 8 were used to built miRNA-mRNA interaction network. Results revealed three and eight key mRNAs and miRNAs, respectively, in this network (Fig. 3;Supplementary Table 14 and Supplementary Table 15). Both SLC7A6OS and FAM126B had the highest degree value among mRNAs, and hsa-miR-31-5p had the highest degree among miRNAs. Besides, other two miRNA-mRNA functional interaction networks were built based on mRNA expression profile 3 and miRNA expression profile 13, mRNA expression profile 13 and miRNA expression profile 3, respectively, and results suggested UBN2, QKI, hsa-miR-27a-3p, hsa-miR-27b-3p, and hsa-miR-3613-3p also played key roles (Supplementary Table 16 to 19; Supplementary Fig. 3 and Supplementary Fig. 4).

RT-qPCR validation

On the basis of mRNA-mRNA-network, STC, and mRNA-miRNA-network analyses results, a representative set of ten mRNAs (PIK3R3, KRAS, CTNNB1, HIF1A, ITGA2, KIT, SOCS3, GNAI3, STAT3 and PTEN) and nine miRNAs (hsa-miR-27a-3p, hsa-miR-27b-3p, hsa-miR-34b-3p, hsa-miR-3613-3p, hsa-miR-575, hsa-miR-8063, hsa-miR-937-5p, hsa-miR-181a-5p and hsa-miR-181b-5p) were selected to make further RT-qPCR validation.

RT-qPCR validation in lung tissues

According to quality-control tests results, there was one excluded normal people lung tissue due to no detection. Finally, a total of ten lung tissues were included in lung tissues RT-qPCR: three of control group, and seven of case group. The results showed that four mRNAs (Fig. 4a) and seven miRNAs (Fig. 4b) expressions were significantly down-regulated when comparing with those of control group: 1) four mRNAs included HIF1A, SOCS3, GNAI3, and PTEN; 2) seven miRNAs included hsa-miR-27a-3p, hsa-miR-27b-3p, hsa-miR-34b-3p, hsa-miR-575, hsa-miR-8063, hsa-miR-937-5p, and hsa-miR-181b-5p. Moreover, PTEN had the most significantly down-regulated expression (P< 0.001),and the lung tissues RT-qPCR results verified those of microarray analyses, except for hsa-miR-575, hsa-miR-8063, and hsa-miR-937-5p.

RT-qPCR validation in blood samples

Similarly, there were 16 blood samples of case group were excluded due to no detection: 11 of mRNAs RT-qPCR, and 5 of miRNAs RT-qPCR; and other 10 blood samples of control groupwere excluded in mRNAs RT-qPCR. As a result, a total of 560 samples were included in mRNAs validation: 393 of case group, and 167 of control group; and 576 samples were included in miRNAs validation: 399 of case group, and 177 of control group. The results indicated that PTEN and GNAI3 expressions were significantly up-regulated (P< 0.001) (Fig. 5a), whereas hsa-miR-8063 and hsa-miR-181b-5p were significantly down-regulated (P< 0.001) (Fig. 5b).

Bisulfite Sequencing PCR (BSP)

On the basis of above results, we randomly selected 54 and 21 blood samples of case and control groups, respectively, to make further bisulfite sequencing PCR (BSP) to detect PTEN methylation rate. The results indicated that PTEN in case group had significantly decreased methylation rate when compared with that of control group (control group: 3.54% ± 0.06, case group: 3.50% ± 0.05, P< 0.01) (Supplementary Table 20).

Discussion

Our study presents a comprehensive analysis of differential mRNA and miRNA expression between silicosis patients and normal people. To our knowledge, this is the first study to report mRNA and miRNA expression on transcriptomic level in lung tissue. The microarray processing and analyses identified aberrant mRNA and miRNA expressions in global scale, and the number of mRNAs with significant expression differences was larger than that of miRNAs. In addition, gene expression function and phagosome pathway were significantly enriched in differential mRNAs expressions, and network analyses revealed nine key mRNAs in mRNA-mRNA-network. Interestingly, PTEN was identified as potential biomarker for silicosis.

Overdose and long-term exposure to silica dust could induce severe lung cells toxicities, including inflammation response[16], extracellular oxidative stress[17], cell apoptosis[18, 19], DNA damage[18, 19], fibrosis[20-22], etc. Dysregulated mRNAs and miRNAs associated with silica-induced pulmonary fibrosis, pneumoconiosis, or silicosis were reported in previous studies[14, 23-27], but the exact identify of differential mRNA and miRNA expression remains to be completely elucidated. Based on silicosis rats model, 39 altered miRNAs were identified involving in lung fibrosis[10]; based on silicosis patients bronchoalveolar lavage fluid (BALF) samples, there were 110 dysregulated miRNAs, and different stages of silicosis were associated with distinct changes in miRNAs expression[4]; whereas our results showed 1417 and 241 differentially expressed mRNAs and miRNAs, respectively, and most mRNAs or miRNAs expressions had no significant difference between early stage and advanced stage silicosis lung tissues. The above differences might possibly be explained by miRNA high conservation, species diversity, and sample size expansion[10]. The only relevant report based on five lung tissues of silicosis patients were conducted to validate decreased miR-486-5p expression[14], and that is consistent with our result. Furthermore, we identified other differentially expressed mRNAs and miRNAs which have not been reported previously.

Our enrichment analyses revealed that differential mRNAs expressions were involved in many functions and signal pathways which were rarely reported in previous studies. Most previous studies showed that inflammation and immune response were mainly involved in silica-exposure induced aberrantly expressed mRNAs and miRNAs[4-6, 8, 9, 13, 28], and these two functions were also observed in our study. Moreover, epithelial-mesenchymal transition (EMT)[23], cell autophagy[27], and alveolar structural damage[26] functions, as well as PI3K/Akt/mTOR/Snail[23], TGF-β1/Smad3[24], and MAPK/ERK[27] signal pathways were associated with the dysregulated mRNAs and miRNAs. For instance, miR-503 was reported to modulate epithelial-mesenchymal transition in silica-induced pulmonary fibrosis by targeting PI3K/Akt/mTOR/Snail pathway[23]. In addition to those, functions like gene expression, viral reproduction, viral infectious cycle, translational initiation, and mRNA metabolic process, as well as signal pathways like phagosome, ribosome, olfactory transduction, and antigen processing and presentation found in this study suggested the need of further study. An unexpected discovery was silica-exposure induced differentially expressed mRNAs were involved in proteoglycans in cancer and pathways in cancer, and this result might reveal a critical link (direct or indirect) between silica exposure and lung cancer[29, 30]. For instance, HIF1A was significantly associated with overall cancer risk[31], especially the lung cancer increased risk[32].

The following RT-qPCR results highlighted the importance of conducting silicosis related transcriptome study in human lung tissue, especially mRNA-related research. Based on lung tissues, RT-qPCR showed HIF1A, SOCS3, GNAI3, PTEN, hsa-miR-27a-3p, hsa-miR-27b-3p, hsa-miR-34b-3p, hsa-miR-575, hsa-miR-937-5p, and hsa-miR-181b-5p expressions were significantly down-regulated. In addition, PTEN had the most significantly down-regulated expression. This result was consistent with our previous study result: silicosis patients lung tissues had abnormal DNA methylation, and PTEN promoter hypermethylation might be associated with decrease of PTEN protein[15]. In addition, hsa-miR-8063 expression in both lung tissues and blood samples was down-regulated, which was not consistent with microarray analysis. This

result might be explained by microarray detection potential limit such as limited representativeness[33]. However, PTEN and GNAI3 expressions were significantly up-regulated in blood samples, and the bisulfite sequencing PCR result demonstrated PTEN had significantly decreased methylation rate in silicosis patients blood samples. Therefore, we speculated that there might be subsequent positive feedback regulation on PTEN decrease: lung tissue PTEN decrease promotes other tissues secrete PTEN into blood, then PTEN transferred from blood into lung tissues. Nevertheless, this study results provided critical reference for better clarifying the detailed biological mechanisms.

The major limitation of this study is the small number of lung tissues samples, precluding to some degree firm conclusions. However, Genome-wide profiling based on silicosis patients and normal people lung tissues is inevitably limited by the small sample size. Besides, microarray-based analysis could not identify sequence variation, and the detection limit of the technology was also depended on the probe and array design[9].

In summary, we conducted a transcriptome study based on human lung tissues and blood samples, and broadened the subjects diversity in silicosis related transcriptome studies. Integrated analysis indicated PTEN hypomethylation could be a biomarker for early detection of silicosis.

Declarations

Data Availability: All data associated with this study are available in the main text or the Supplementary Materials.

Acknowledgements: We are sincerely grateful to the staff of the Chinese Center for Disease Control and Prevention.

Author Contributions: Conceptualization, Meng Ye, Daoyuan Sun and Weijiang Hu; methodology,Kai Liu and Meng Ye; software, Kai Liu and Weijiang Hu; validation, Meng Ye and Xin Sun; resources, Weijiang Hu, Jingbo Zhang, Jie Liu, Yuxin Zheng, Liangying Mei, Zushu Qian, Qiangguo Sun, Qiang Liu, Zhijun Wu, Hengdong Zhang, Yanping Li; data curation, Jingbo Zhang; writing—original draft preparation, Kai Liu; writing—review and editing, Meng Ye, Daoyuan Sun and Jingbo Zhang; supervision, Meng Ye and Daoyuan Sun; project administration, Meng Ye; funding acquisition, Meng Ye and Daoyuan Sun. All authors have read and agreed to the published version of the manuscript.

Competing Financial Interests statement: The authors declare no competing interests.

Funding: This research was funded by grants of National Natural Science Foundation of China (81472956, 30972449), and by Domestic Cooperation Projects of Shanghai Science and Technology Commission of China (20015800300), Professor Sun Daoyuan occupational disease expert team of Shanghai Pulmonary Hospital Affiliated to Tongji University (SZYJTD201904) and also supported by the Occupational health risk assessment and national occupational health standard setting project

(131031109000150003) of National Institute for Occupation Health and Poison Control, Chinese Center for Disease Control and Prevention.

Role of the Funder/Sponsor: the Funder/Sponsor had no role in sample collection, data management, analysis or interpretation in this study.

Institutional Review Board Statement: The study was conducted according to the guidelines of the Declaration of Helsinki, and approved by the Ethics Committee Board in Occupational Health and Poison Control, Chinese Center for Disease Control and Prevention (protocol code 201402 and date of approval, March 3, 2014).

Informed Consent Statement: Informed consent was obtained from all subjects involved in the study.

References

[1] Shi, P., Xing, X., Xi, S., Jing, H., Yuan, J. and Fu, Z. et al. (2020) Trends in global, regional and national incidence of pneumoconiosis caused by different aetiologies: an analysis from the Global Burden of Disease Study 2017. *OCCUP ENVIRON MED*, **77**, 407-414.

[2] The, L.R.M. (2019) The world is failing on silicosis. *Lancet Respir Med*, **7**, 283.

[3] Rao, K.M., Porter, D.W., Meighan, T. and Castranova, V. (2004) The sources of inflammatory mediators in the lung after silica exposure. *Environ Health Perspect*, **112**, 1679-1686.

[4] Zhang, Y., Wang, F., Zhou, D., Ren, X., Zhou, D. and Gao, X. et al. (2016) Genome-wide analysis of aberrantly expressed microRNAs in bronchoalveolar lavage fluid from patients with silicosis. *IND HEALTH*, **54**, 361-369.

[5] Chen, J., Yao, Y., Su, X., Shi, Y., Song, X. and Xie, L. et al. (2018) Comparative RNA-Seq transcriptome analysis on silica induced pulmonary inflammation and fibrosis in mice silicosis model. *J APPL TOXICOL*, **38**, 773-782.

[6] Zhou, Y., He, L., Liu, X.D., Guan, H., Li, Y. and Huang, R.X. et al. (2019) Integrated Analysis of lncRNA and mRNA Transcriptomes Reveals New Regulators of Ubiquitination and the Immune Response in Silica-Induced Pulmonary Fibrosis. *BIOMED RES INT*, **2019**, 6305065.

[7] Yang, Z., Li, Q., Yao, S., Zhang, G., Xue, R. and Li, G. et al. (2016) Down-Regulation of miR-19a as a Biomarker for Early Detection of Silicosis. *Anat Rec (Hoboken)*, **299**, 1300-1307.

[8] Chan, J., Tsui, J., Law, P., So, W., Leung, D. and Sham, M. et al. (2017) Profiling of the silica-induced molecular events in lung epithelial cells using the RNA-Seq approach. *J APPL TOXICOL*, **37**, 1162-1173.

[9] Chan, J., Tsui, J., Law, P., So, W., Leung, D. and Sham, M. et al. (2018) RNA-Seq revealed ATF3-regulated inflammation induced by silica. *TOXICOLOGY*, **393**, 34-41.

[10] Faxuan, W., Qin, Z., Dinglun, Z., Tao, Z., Xiaohui, R. and Liqiang, Z. et al. (2012) Altered microRNAs expression profiling in experimental silicosis rats. *J TOXICOL SCI*, **37**, 1207-1215.

[11] Xu, T., Yan, W., Wu, Q., Xu, Q., Yuan, J. and Li, Y. et al. (2019) MiR-326 Inhibits Inflammation and Promotes Autophagy in Silica-Induced Pulmonary Fibrosis through Targeting TNFSF14 and PTBP1. *CHEM RES TOXICOL*, **32**, 2192-2203.

[12] Zhang, Y., Wang, F., Lan, Y., Zhou, D., Ren, X. and Zhao, L. et al. (2015) Roles of microRNA-146a and microRNA-181b in regulating the secretion of tumor necrosis factor-alpha and interleukin-1beta in silicon dioxide-induced NR8383 rat macrophages. *MOL MED REP*, **12**, 5587-5593.

[13] Zhao, H., Jiang, Z., Lv, R., Li, X., Xing, Y. and Gao, Y. et al. (2020) Transcriptome profile analysis reveals a silica-induced immune response and fibrosis in a silicosis rat model. *TOXICOL LETT*, **333**, 42-48.

[14] Ji, X., Wu, B., Fan, J., Han, R., Luo, C. and Wang, T. et al. (2015) The Anti-fibrotic Effects and Mechanisms of MicroRNA-486-5p in Pulmonary Fibrosis. *Sci Rep*, **5**, 14131.

[15] Zhang, X., Jia, X., Mei, L., Zheng, M., Yu, C. and Ye, M. (2016) Global DNA methylation and PTEN hypermethylation alterations in lung tissues from human silicosis. *J THORAC DIS*, **8**, 2185-2195.

[16] Benmerzoug, S., Rose, S., Bounab, B., Gosset, D., Duneau, L. and Chenuet, P. et al. (2018) STING-dependent sensing of self-DNA drives silica-induced lung inflammation. *NAT COMMUN*, **9**, 5226.

[17] Zelko, I.N., Zhu, J. and Roman, J. (2018) Role of SOD3 in silica-related lung fibrosis and pulmonary vascular remodeling. *Respir Res*, **19**, 221.

[18] Nazarparvar-Noshadi, M., Ezzati, N.D.J., Rasoulzadeh, Y., Mohammadian, Y. and Shanehbandi, D. (2020) Apoptosis and DNA damage induced by silica nanoparticles and formaldehyde in human lung epithelial cells. *Environ Sci Pollut Res Int*, **27**, 18592-18601.

[19] Shifeng, L., Hong, X., Xue, Y., Siyu, N., Qiaodan, Z. and Dingjie, X. et al. (2019) Ac-SDKP increases alpha-TAT 1 and promotes the apoptosis in lung fibroblasts and epithelial cells double-stimulated with TGF-beta1 and silica. *Toxicol Appl Pharmacol*, **369**, 17-29.

[20] Li, C., Du S, Lu, Y., Lu, X., Liu, F. and Chen, Y. et al. (2016) Blocking the 4-1BB Pathway Ameliorates Crystalline Silica-induced Lung Inflammation and Fibrosis in Mice. *THERANOSTICS*, **6**, 2052-2067.

[21] Sugimoto, N., Suzukawa, M., Nagase, H., Koizumi, Y., Ro, S. and Kobayashi, K. et al. (2019) IL-9 Blockade Suppresses Silica-induced Lung Inflammation and Fibrosis in Mice. *Am J Respir Cell Mol Biol*, **60**, 232-243.

[22] Scabilloni, J.F., Wang, L., Antonini, J.M., Roberts, J.R., Castranova, V. and Mercer, R.R. (2005) Matrix metalloproteinase induction in fibrosis and fibrotic nodule formation due to silica inhalation. *Am J*

Physiol Lung Cell Mol Physiol, **288**, L709-L717.

[23] Yan, W., Wu, Q., Yao, W., Li, Y., Liu, Y. and Yuan, J. et al. (2017) MiR-503 modulates epithelial-mesenchymal transition in silica-induced pulmonary fibrosis by targeting PI3K p85 and is sponged by lncRNA MALAT1. *Sci Rep*, **7**, 11313.

[24] Wu, Q., Han, L., Yan, W., Ji, X., Han, R. and Yang, J. et al. (2016) miR-489 inhibits silica-induced pulmonary fibrosis by targeting MyD88 and Smad3 and is negatively regulated by lncRNA CHRF. *Sci Rep*, **6**, 30921.

[25] Chu, M., Ji, X., Chen, W., Zhang, R., Sun, C. and Wang, T. et al. (2014) A genome-wide association study identifies susceptibility loci of silica-related pneumoconiosis in Han Chinese. *HUM MOL GENET*, **23**, 6385-6394.

[26] Yuan, J., Li, P., Pan, H., Li, Y., Xu, Q. and Xu, T. et al. (2018) miR-542-5p Attenuates Fibroblast Activation by Targeting Integrin alpha6 in Silica-Induced Pulmonary Fibrosis. *INT J MOL SCI*, **19**.

[27] Han, R., Ji, X., Rong, R., Li, Y., Yao, W. and Yuan, J. et al. (2016) MiR-449a regulates autophagy to inhibit silica-induced pulmonary fibrosis through targeting Bcl2. *J Mol Med (Berl)*, **94**, 1267-1279.

[28] Zhou, Y., He, L., Liu, X.D., Guan, H., Li, Y. and Huang, R.X. et al. (2019) Integrated Analysis of lncRNA and mRNA Transcriptomes Reveals New Regulators of Ubiquitination and the Immune Response in Silica-Induced Pulmonary Fibrosis. *BIOMED RES INT*, **2019**, 6305065.

[29] Sato, T., Shimosato, T. and Klinman, D.M. (2018) Silicosis and lung cancer: current perspectives. *Lung Cancer (Auckl)*, **9**, 91-101.

[30] Poinen-Rughooputh, S., Rughooputh, M.S., Guo, Y., Rong, Y. and Chen, W. (2016) Occupational exposure to silica dust and risk of lung cancer: an updated meta-analysis of epidemiological studies. *BMC PUBLIC HEALTH*, **16**, 1137.

[31] Anam, M.T., Ishika, A., Hossain, M.B. and Jesmin (2015) A meta-analysis of hypoxia inducible factor 1-alpha (HIF1A) gene polymorphisms: association with cancers. *Biomark Res*, **3**, 29.

[32] Xu, S. and Ying, K. (2020) Association between HIF-1alpha gene polymorphisms and lung cancer: A meta-analysis. *Medicine (Baltimore)*, **99**, e20610.

[33] Quagliata, L., Schlageter, M., Quintavalle, C., Tornillo, L. and Terracciano, L.M. (2014) Identification of New Players in Hepatocarcinogenesis: Limits and Opportunities of Using Tissue Microarray (TMA). *Microarrays (Basel)*, **3**, 91-102.

[34] ILO: Guidelines for the use of the ILO International Classification of Radiographs of Pneumoconioses, Revised edition 2011. Occupational Safety and Health Series No. 22 (Rev.2011). Geneva: International Labour Office 2011.

[35] Polineni, D., Dang, H., Gallins, P.J., Jones, L.C., Pace, R.G. and Stonebraker, J.R. et al. (2018) Airway Mucosal Host Defense Is Key to Genomic Regulation of Cystic Fibrosis Lung Disease Severity. *Am J Respir Crit Care Med*, **197**, 79-93.

[36] Chang, K.H., Chuang, T.J., Lyu, R.K., Ro, L.S., Wu, Y.R. and Chang, H.S. et al. (2012) Identification of gene networks and pathways associated with Guillain-Barre syndrome. *PLOS ONE*, **7**, e29506.

[37] Geng, W., Zhou, G., Zhao, B., Xiao, Q., Li, C. and Fan, S. et al. (2020) Liquiritigenin suppresses the activation of hepatic stellate cells via targeting miR-181b/PTEN axis. *PHYTOMEDICINE*, **66**, 153108.

[38] Jin, H., Li, C., Dong, P., Huang, J., Yu, J. and Zheng, J. (2020) Circular RNA cMTO1 Promotes PTEN Expression Through Sponging miR-181b-5p in Liver Fibrosis. *Front Cell Dev Biol*, **8**, 714.

Figures

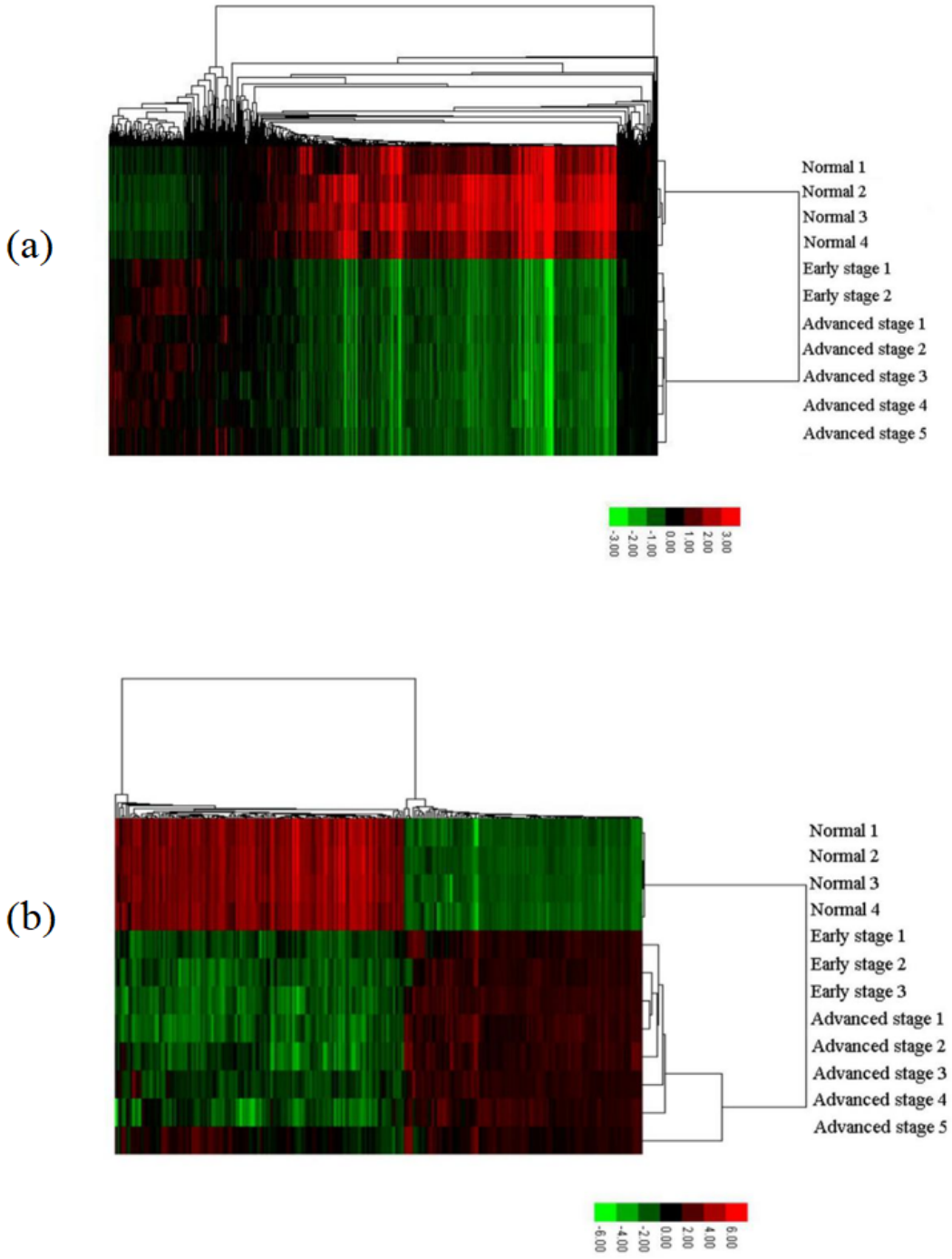

Figure 1

a Hierarchical cluster of mRNA profiles. Every row represents one tissue sample: normal 1 to 4 represent normal lung tissues, early stage 1 and 2 represent early stage silicosis tissues, and advanced stage 1 to 5 represent advanced stage silicosis tissues. Every column represents one mRNA/miRNA probe. Red color indicates over-expression, and green indicates low-expression. The threshold of significance was P value < 0.05. b Hierarchical cluster of miRNA (b) profiles. Every row represents one tissue sample: normal 1 to 4

represent normal lung tissues, early stage 1 to 3 represent early stage silicosis tissues, and advanced stage 1 to 5 represent advanced stage silicosis tissues. Every column represents one mRNA/miRNA probe. Red color indicates over-expression, and green indicates low-expression. The threshold of significance was P value < 0.05.

(a)

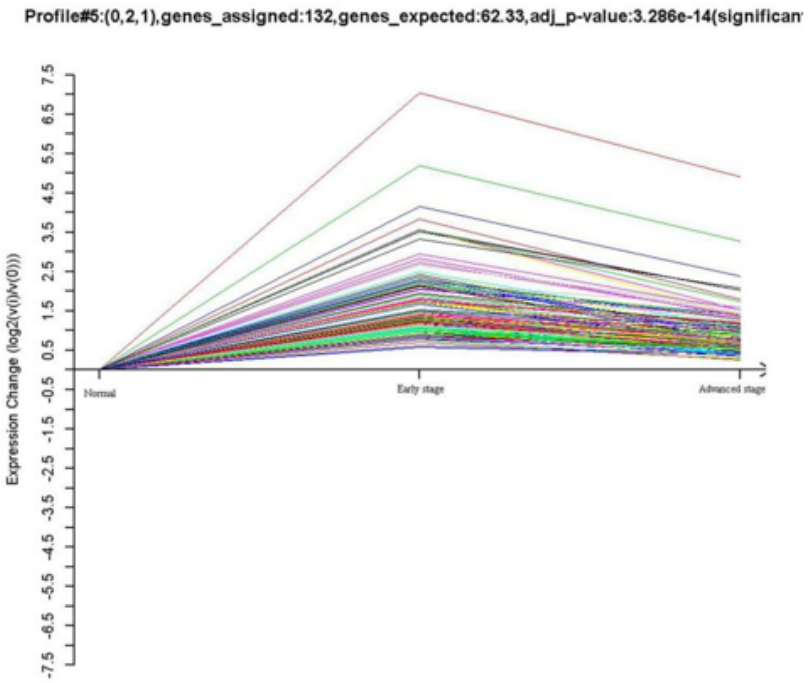

(b)

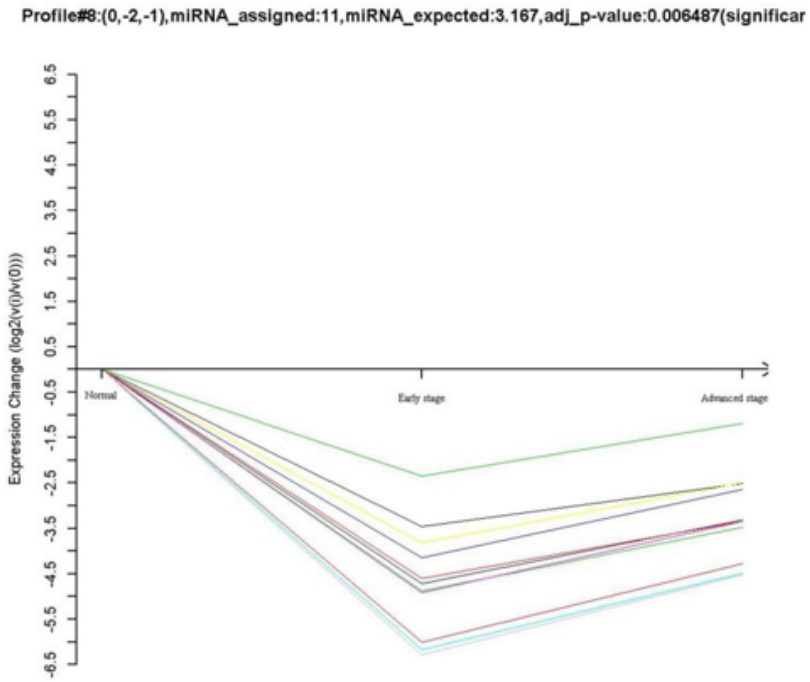

Figure 2

a Detailed trends of mRNA expression profile 5.The horizontal axis represents different lung tissues: normal lung, early stage silicosis, advanced stage silicosis; and their vertical axis represents raw expression values that are converted into log2 ratio. b Detailed trends of miRNA expression profile 8 (b).The horizontal axis represents different lung tissues: normal lung, early stage silicosis, advanced stage silicosis; and their vertical axis represents raw expression values that are converted into log2 ratio.

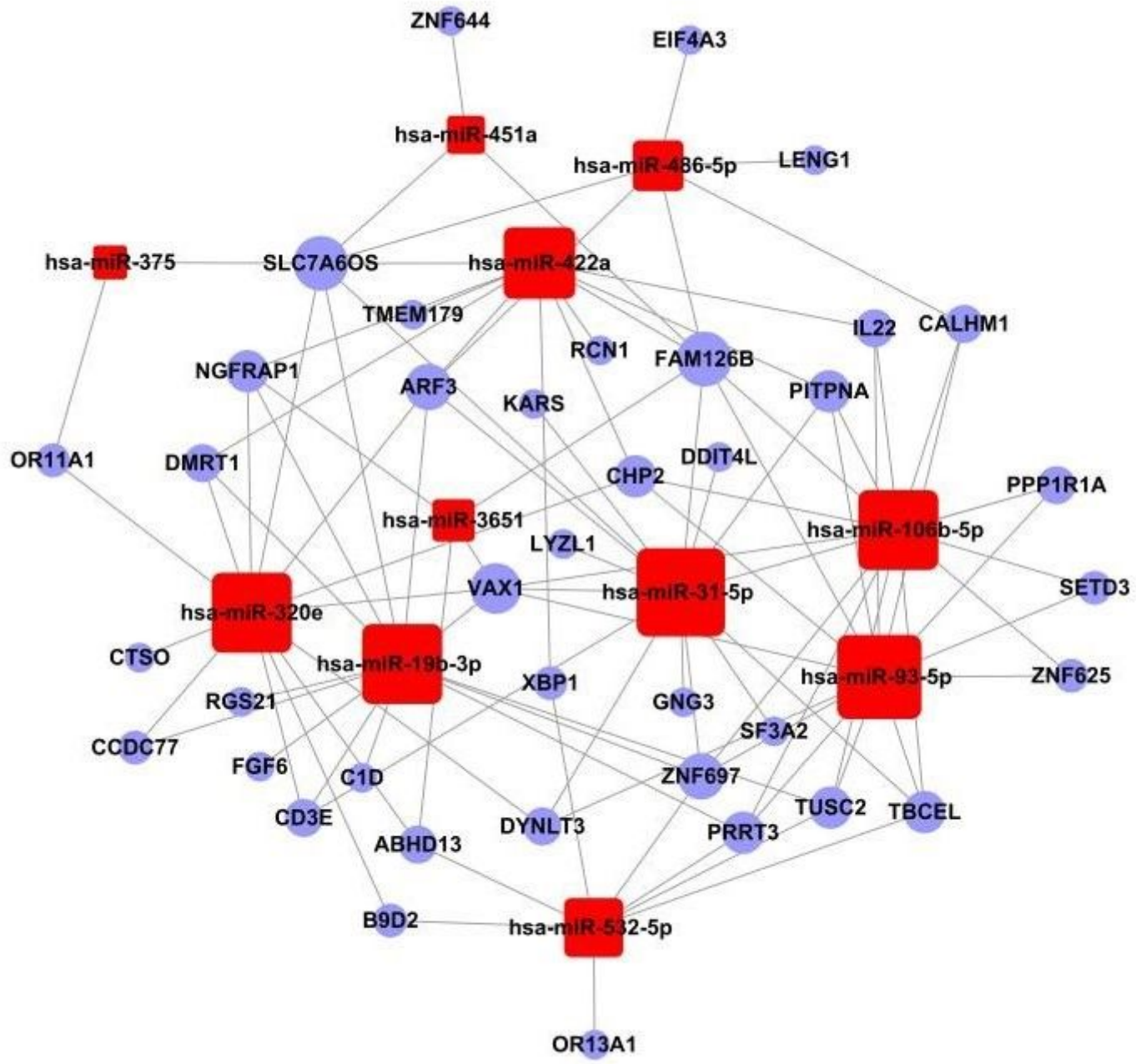

Figure 3

miRNA-mRNA-network. Square represents microRNA, node represents mRNA, and straight line represents regulatory relationship between microRNA and mRNA.

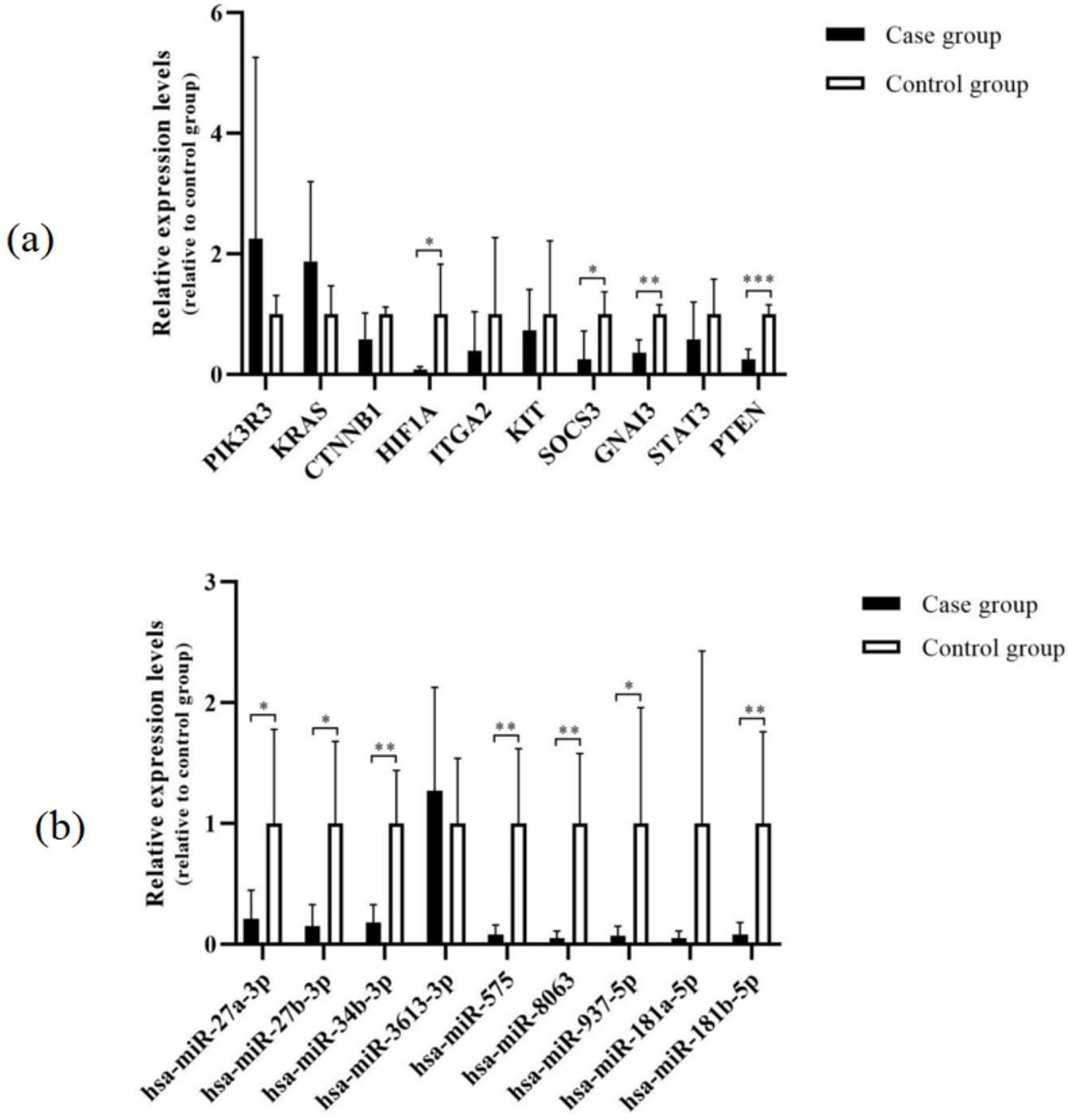

Figure 4

a RT-qPCR analyses of mRNAs relative expression levels based on lung tissues.Data show mean ± standard deviation, and the above asterisks between control and case groups represent statistical significance (unpaired two-tailed Student's t-test):*P < 0.05, **P < 0.01, ***P < 0.001. b RT-qPCR analyses of miRNAs (b) relative expression levels based on lung tissues. Data show mean ± standard deviation,

and the above asterisks between control and case groups represent statistical significance (unpaired two-tailed Student's t-test):*P < 0.05, **P < 0.01, ***P < 0.001.

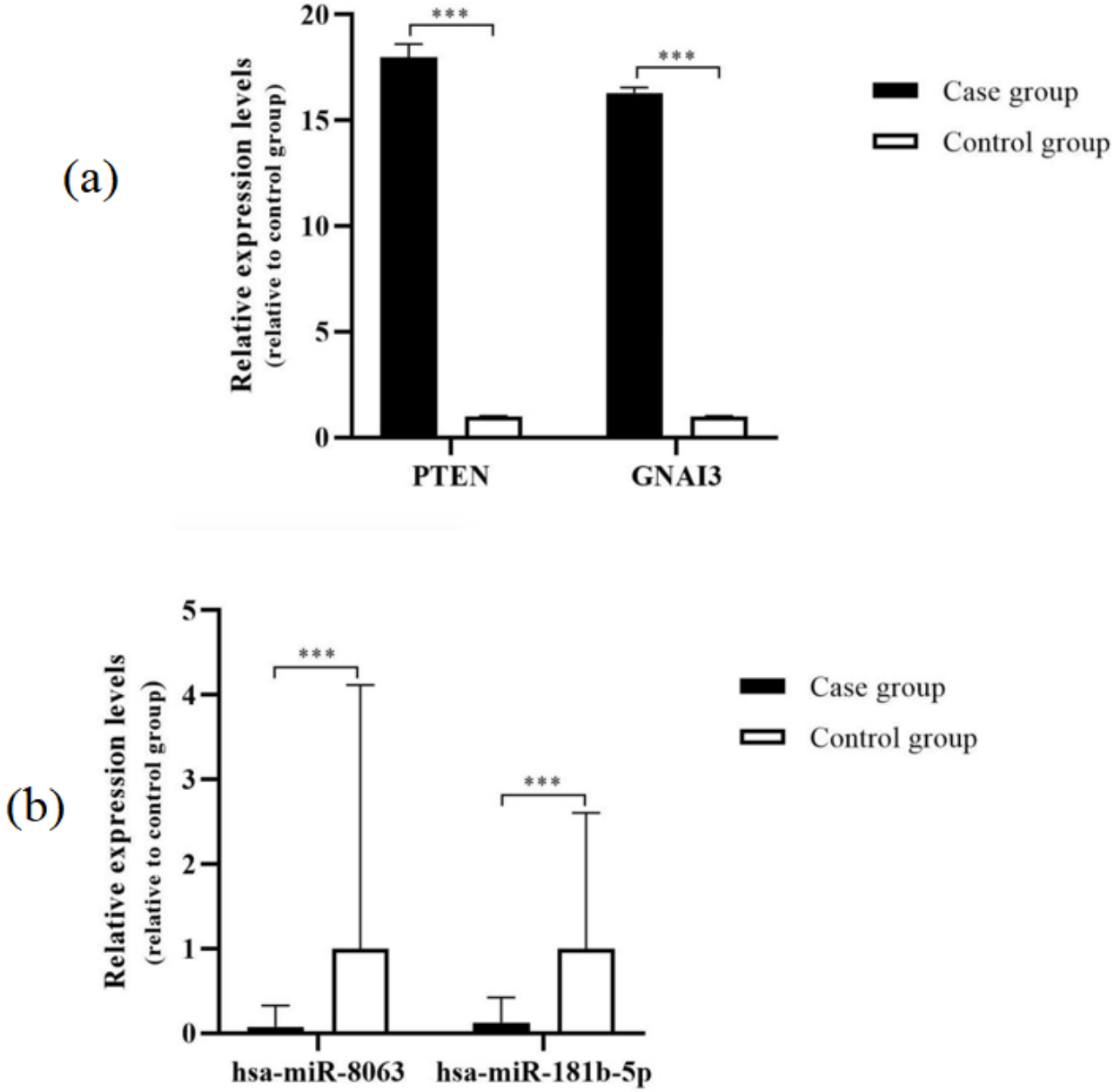

Figure 5

a RT-qPCR analyses of further selected mRNAs relative expression levels based on blood samples. Data show mean ± standard deviation, and the above asterisks between control and case groups represent statistical significance (unpaired two-tailed Student's t-test): *P < 0.05, **P < 0.01, ***P < 0.001. b RT-qPCR analyses of further selected miRNAs (b) relative expression levels based on blood samples. Data show

mean ± standard deviation, and the above asterisks between control and case groups represent statistical significance (unpaired two-tailed Student's t-test): *P < 0.05, **P < 0.01, ***P < 0.001.

Supplementary Files

This is a list of supplementary files associated with this preprint. Click to download.

- Supplementaryfiles.zip